

ChemComm

Accepted Manuscript



This is an *Accepted Manuscript*, which has been through the Royal Society of Chemistry peer review process and has been accepted for publication.

Accepted Manuscripts are published online shortly after acceptance, before technical editing, formatting and proof reading. Using this free service, authors can make their results available to the community, in citable form, before we publish the edited article. We will replace this *Accepted Manuscript* with the edited and formatted *Advance Article* as soon as it is available.

You can find more information about *Accepted Manuscripts* in the [Information for Authors](#).

Please note that technical editing may introduce minor changes to the text and/or graphics, which may alter content. The journal's standard [Terms & Conditions](#) and the [Ethical guidelines](#) still apply. In no event shall the Royal Society of Chemistry be held responsible for any errors or omissions in this *Accepted Manuscript* or any consequences arising from the use of any information it contains.



Journal Name

COMMUNICATION

Mixed-linker Approach in Designing Porous Zirconium Based Metal-Organic Frameworks with High Hydrogen Storage Capacity

Received 00th January 20xx,
Accepted 00th January 20xx

Ayesha Naeem,^a Valeska P. Ting,^b Ulrich Hintermair,^b Mi Tian,^b Richard Telford,^a Saaiba Halim,^a Harriott Nowell,^c Małgorzata Holyńska,^d Simon J. Teat,^e Ian J. Scowen^f and Sanjit Nayak^{a*}

DOI: 10.1039/x0xx00000x

www.rsc.org/

Three highly porous Zr(IV) based metal-organic frameworks, UBMOF-8, UBMOF-9, and UBMOF-31 were synthesized by using 2,2'-diamino-4,4'-stilbenedicarboxylic acid, 4,4'-stilbenedicarboxylic acid, and combination of both linkers, respectively. The mixed-linker UBMOF-31 shows excellent hydrogen uptake of 4.9 wt% and high selectivity for adsorption of CO₂ over N₂ with high thermal and moderate water stability with permanent porosity and surface area of 2552 m² g⁻¹.

Hydrogen has gained enormous attention as promising energy vector in renewable energy conversion schemes due to its environment friendly nature; it can be cleanly produced by electrolysis of water, and water is the main by-product of H₂ combustion.¹ However, especially for applications in automobiles, storage and transportation of hydrogen is a major challenge due to its very low boiling point and low volumetric density in gaseous form.²⁻⁴ Metal-organic frameworks (MOFs) with very high surface areas are promising candidates for tackling this problem by adsorptive storage of hydrogen to achieve higher hydrogen densities at acceptable conditions.⁵⁻⁸ Research in this area has indicated that this class of materials has the potential for meeting the systems storage capacity benchmark of 5.5 wt% of H₂ set for 2017 by the US Department of Energy (DOE).⁹ Despite the large number of MOFs studied for hydrogen storage properties,^{2, 6, 8, 10, 11} the problem of low thermal and water stabilities of many MOFs is

a major issue for practical applications.¹² Newly developed Zr-based MOFs with archetypical [Zr₆O₄(OH)₄(CO₂)] secondary building units (SBUs) are highly promising for this purpose, due to their exceptional thermal and water stabilities,¹³⁻¹⁶ and recent studies have shown that UiO-67 (UiO: University of Oslo) can reach up to 4.6 wt% H₂ storage at 3.8 MPa.¹⁴

Here we report three Zr(IV) based MOFs using 4,4'-stilbenedicarboxylic acid and 2,2'-diamino-4,4'-stilbenedicarboxylic acid as linkers, with one of them synthesized using non-traditional mixed-linker approach, showing one of the highest (up to 4.9 wt%) measured hydrogen uptakes among the Zr-based MOFs reported to date.^{14, 15, 17, 18} In addition, high selectivity of CO₂ adsorption over nitrogen was also observed for UBMOF-31. Solvothermal reactions of 2,2'-diamino-4,4'-stilbenedicarboxylic acid (DASDCAH₂) and 4,4'-stilbenedicarboxylic (SDCAH₂) acid with ZrCl₄ and benzoic acid (modulator) in a mixture of dimethylformamide (dmf) and N-methyl-2-pyrrolidone (NMP) (5:1, v/v) produced [Zr₆O₄(OH)₄(DASDCA)₆](PhCOOH)_m(dmf)_x(H₂O)_y(NMP)_z (UBMOF-8), and [Zr₆O₄(OH)₄(SDCA)₆](PhCOOH)_n(dmf)_p(H₂O)_q(NMP)_r (UBMOF-9), respectively, where UBMOF refers to University of Bradford Metal-Organic Framework (Figure 1).¹⁹ The actual amount of solvent in the lattice varies, and was not determined experimentally for these compounds. Both of these syntheses resulted in crystals suitable for structural analysis by single crystal X-ray diffraction. Both of these MOFs are formed of octahedral [Zr₆O₄(OH)₄(CO₂)] cluster units connected by twelve DASDCA or SDCA linkers similar to UiO-66.¹³ Use of these longer linkers results into large diagonal cage dimensions of approximately 25 Å and equilateral triangular faces with 17.7 Å side lengths (Figure 1 and Figure S3.1 in ESI). Structural analyses using OLEX-2 program suite indicate 71.9 % and 75.3 % solvent accessible volumes for UBMOF-8, and UBMOF-9, respectively, with a probe of 1.2 Å radius.²⁰

Unlike UBMOF-9, UBMOF-8 did not produce a phase pure material despite extensive efforts to optimise the synthetic conditions. An unidentified amorphous phase was present alongside the crystalline material for UBMOF-8 (Figure 2), as

^a School of Chemistry and Forensic Sciences, University of Bradford, Richmond Road, Bradford, West Yorkshire, BD7 1DP, United Kingdom

^b Department of Chemical Engineering, University of Bath, Claverton Down, Bath, BA2 7AY, UK

^c Diamond Light Source, Didcot, Oxon, OX11 0DE, UK

^d Fachbereich Chemie und Wissenschaftliches Zentrum für Materialwissenschaften, Philipps Universität Marburg, Hans-Meerwein-Straße, 35043 Marburg, Germany

^e Advance Light Source, Lawrence Berkeley National Laboratory, Berkeley, CA 94720 USA

^f School of Chemistry, University of Lincoln, Brayford Pool, Lincoln, Lincolnshire, LN6 7TS, United Kingdom

Electronic Supplementary Information (ESI) available: Experimental details, single-crystal structure determination, materials characterization (IR, TGA, NMR), and details of gas sorption experiments. CCDC reference numbers 1440758 and 1440759 for UBMOF-8 and UBMOF-9, respectively. For ESI and crystallographic data in CIF or other electronic format see DOI: 10.1039/x0xx00000x

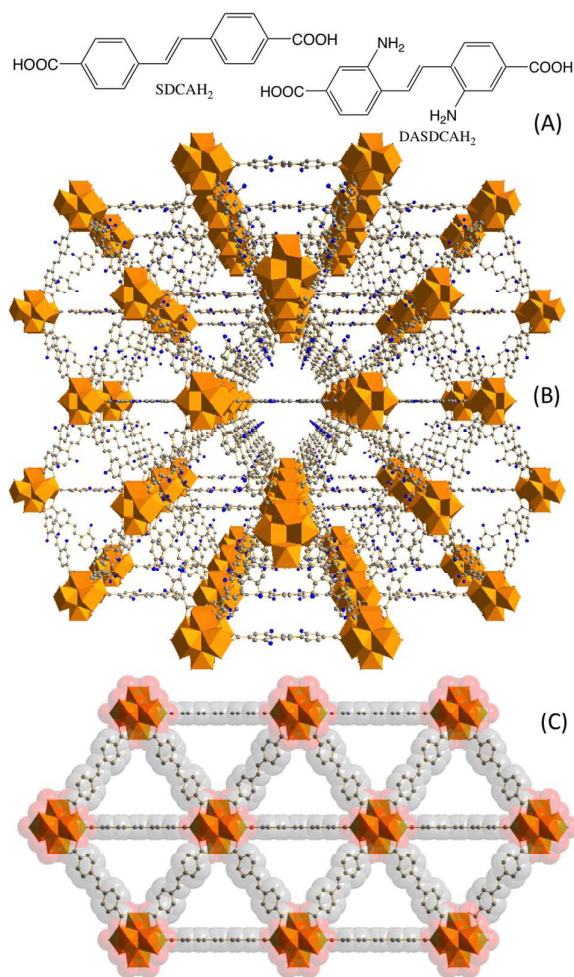


Figure 1. (A) The two linkers, 2,2'-diamino-4,4'-stilbenedicarboxylic acid (DASDCAH₂) and 4,4'-stilbenedicarboxylic (SDCAH₂) acid, used to synthesise UBMOF-8 and UBMOF-9, respectively. (B) Central projection view of UBMOF-8 along 101 (hkl) direction. (C) Crystallographic view of UBMOF-8 along 101 (hkl) with [Zr₆O₈] polyhedral nodes shown in orange to demonstrate three-dimensional porosity of the structures. The hydrogen atoms and the disordered carbon and nitrogen atoms are excluded for clarity.

evidenced by a noticeable amorphous halo in the PXRD pattern (Figure 3A). As an alternate route to access the pure isostructural MOF with amino groups we took advantage of the similar coordination behaviour of both linkers, and experimentally optimised the ratio of two linkers. This mixed linker approach resulted into a crystalline phase pure material (UBMOF-31) isostructural to UBMOF-8 and UBMOF-9 when DASDCAH₂ and SDCAH₂ were used in 1:2.5 molar ratios. The empirical formula for desolvated UBMOF-31, [Zr₆O₄(OH)₄(DASDCA)_{1.4}(SDCA)_{4.6}] (PhCOOH)_{0.78}, was determined from combination of data obtained from elemental analysis, thermogravimetric analysis (TGA) and NMR spectroscopy (see Electronic Supporting Information (ESI) for details).

The calculated and measured PXRD patterns match closely, suggesting a phase pure crystalline material for the pristine sample for UBMOF-9 (Figure 3B). The single crystals of UBMOF-8 produced along with powdery amorphous materials can be observed in the SEM images (see ESI). The discrepancy

of elemental analysis (see ESI) for UBMOF-8 further suggests the presence of impurity in the bulk material. The residual amounts of modulator (PhCOOH) inside the MOFs were estimated for the solvent exchanged and dried samples (see ESI). In the IR spectra the presence of the C=O stretching frequency (1685 cm⁻¹) for non-coordinate benzoic acid indicates their origin as guest molecules, not from defects. The flexibility of the linkers possibly play a role in minimizing defects for this class of MOFs, as was observed for another family of isostructural Zr-based MOFs with varied flexibility.²¹ In addition, the presence of extensive disorder in the crystal structures restricts the estimation of any further investigation on accurate determination of defects in these materials.²² It is evident from literature that the presence of amino groups on the linkers facilitates hydrogen adsorption in MOFs.²³ This motivated us to explore an alternate route to produce a phase pure amino functionalized isostructural MOF by mixed-linker approach with controlled use of both linkers to synthesise UBMOF-31 with the DASDCAH₂:SDCAH₂ ratio of 1.4:4.6. Further increase of DASDCAH₂ resulted in the amorphous impurity as originally observed for UBMOF-8. Infrared spectra (see ESI) for all three fresh compounds indicate the presence of large amount of dmf with an intense peak at 1654 cm⁻¹, which diminished upon washing with acetone, and activation by supercritical CO₂ during gas adsorption studies. The presence of the shoulder peaks around 3670 cm⁻¹ possibly originates from the OH groups as suggested in literature.²⁴ Thermal stabilities of the three MOFs were studied by TGA in air (see ESI) at a 5 °C per minute heating ramp. All three freshly prepared, air-dried MOFs show a large initial drop in weight (40% to 50%) due to solvent loss, followed by a stable plateau until they decompose at approximately 494 °C (UBMOF-8), 522 °C (UBMOF-9), and 508 °C (UBMOF-31), indicating thermal stabilities comparable with UiO-66.^{13, 14} TGA of de-solvated and vacuum treated samples were analysed to estimate the linker ratio for UBMOF-31 and guest modulator, in combination with elemental analysis and NMR spectroscopy (see ESI). The PXRD pattern in Figure 3A suggests that UBMOF-31 is phase pure and isostructural to UBMOF-8 and UBMOF-9 as expected. PXRD analyses of the samples revealed the

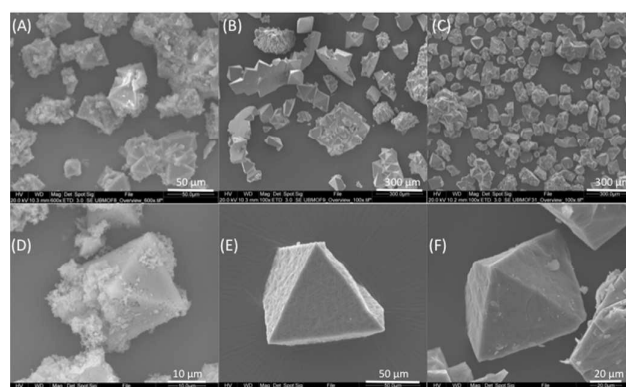


Figure 2. SEM images of bulk phases of (A) UBMOF-8, (B) UBMOF-9, (C) UBMOF-31 and their close up views D, E, and F, respectively.

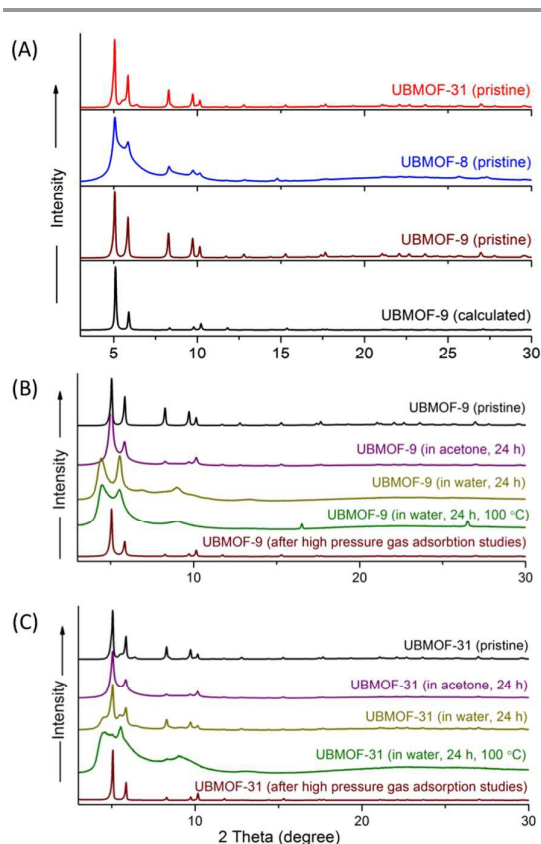


Figure 3. (A) Calculated PXRD pattern for UBMOF-9 and measured PXRD patterns for pristine UBMOF-8, UBMOF-9, and UBMOF-31 suggesting the phase-pure bulk material for UBMOF-9 and UBMOF-31. (B, C) Comparison of PXRD patterns of UBMOF-9, and UBMOF-31 treated at different conditions.

stability of UBMOF-9 and UBMOF-31 under different conditions as shown in Figure 3. Both of these materials retain their original structure when treated in acetone for 24 hours at 20 °C, after activation using supercritical CO₂, and after high-pressure adsorption studies with N₂, H₂, and CO₂. When treated in water at 20 °C for 24 hours, both (UBMOF-8 and UBMOF-31) retain their shiny crystalline morphology to some extent as visually inspected (see ESI) and evidenced by PXRD (Figure 3), with a small shift in 2θ for the low angle peaks for UBMOF-9. However, UBMOF-31 mostly retains its original PXRD pattern, indicating better water-stability compared to UBMOF-9. Hydrothermal treatment (100 °C) of both of the MOFs over 24 hours resulted in broadening of the low angle peaks leaving no visible high-angle peaks, indicating significant loss of crystallinity of the materials. The surface areas of the materials were determined using Brunauer-Emmett-Teller (BET) analysis with N₂ at 77 K on a Micromeritics 3-Flex volumetric gas sorption analyser (P/P₀ range 0.05-0.3) following the British Standard guidelines.²⁵ A sample of UBMOF-9 that had been solvent-exchanged with acetone and degassed at 150 °C for 8 hours under dynamic high vacuum (10⁻⁷ mbar) prior to analysis displayed a surface area of 1169 m²g⁻¹. In order to access the true intrinsic porosity of these materials, samples were solvent exchanged and subsequently subjected to supercritical CO₂ (scCO₂) extraction.^{26, 27} The scCO₂-activated samples showed BET surface areas of 2667

m²g⁻¹ and 2552 m²g⁻¹ for UBMOF-9 and UBMOF-31, respectively, more than twice the value obtained for the thermally dried samples. High pressure gas sorption analysis for both of scCO₂-activated MOFs was carried out. A maximum loading of ~4 wt% was observed for UBMOF-9 at our measured range of 13 MPa without reaching saturation (Figure 4A). In contrast, UBMOF-31 reaches maximum uptake of 4.9 wt% at 4.6 MPa at 77 K (Figure 4A), making it one of the best Zr-based MOFs for hydrogen storage capacity to date.¹⁴ The presence of a maximum observed for UBMOF-31 is usual and expected where the surface interacts positively for the adsorption process, and adsorption efficiency drops after covering the surface with the first layer of guest molecules.^{8, 28} For a brief overview and comparison of hydrogen uptake by different Zr-based MOFs see the Table S8.1 in ESI. The increased hydrogen storage capacity of UBMOF-31 can be explained by attractive interaction between the H₂ molecules and the amino substituted benzene rings as suggested by theoretical calculations.²³

Despite a large number of MOFs with high selectivity towards CO₂ adsorption, only a few of them are stable under air and moisture, restricting their possible applications in CO₂ capture and separation.¹² In addition, presence of amino groups on the linkers often facilitates CO₂ adsorption by chemisorption process. The presence of both of these features motivated us further to study CO₂ adsorption properties for these MOFs.²⁹ The CO₂ uptake was recorded 8 wt% and 8.6 wt% for UBMOF-9 and UBMOF-31, respectively at 0 °C and 1 bar pressure. Slightly lower uptake of 2.06 wt% and 2.86 wt% were observed for UBMOF-9 and UBMOF-31, respectively at 20 °C and 1 bar pressure (Figure S8.9 in ESI). Adsorption of CO₂ under high pressure was also studied. Notably UBMOF-31 shows much greater affinity towards CO₂ reaching 73 wt% compared to 63 wt% for UBMOF-9 at 1MPa (Figure 4B).²⁹ However, at higher pressure, CO₂ uptake for UBMOF-9 exceeds the value for UBMOF-31 (see ESI). Therefore, the first part of the adsorption isotherm is most likely to be dominated by chemisorption at the amine sites, and the latter part by physisorption on the internal surface of the highly porous framework. Consistent with this interpretation, a high selectivity towards CO₂ adsorption over nitrogen was observed, (15:1) for UBMOF-31, in the chemisorption regime at 0 °C and 1 MPa, making it a promising material for CO₂ capture and separation.

In summary, we report three new Zr-based MOFs, UBMOF-8, UBMOF-9, and UBMOF-31 with the latter synthesized using mixed-linker strategy. With presence of amino groups in UBMOF-31, it shows enhanced H₂ adsorption capacity with 4.9 wt% of loading at 4.6 MP, one of the highest uptakes for Zr-based MOFs reported to date. In addition, UBMOF-31 shows high affinity towards CO₂ adsorption over nitrogen, with a selectivity of 15:1 at 0 °C under 1 MPa of pressure. In addition to its exceptional hydrogen uptake, and selectivity towards CO₂ adsorption, UBMOF-31 shows good hydrolytic stability, making it a promising candidate for further studies and practical applications for gas storage and separation. We are currently working on synthesizing phase pure UBMOF-8 and isostructural materials with an increased proportion of

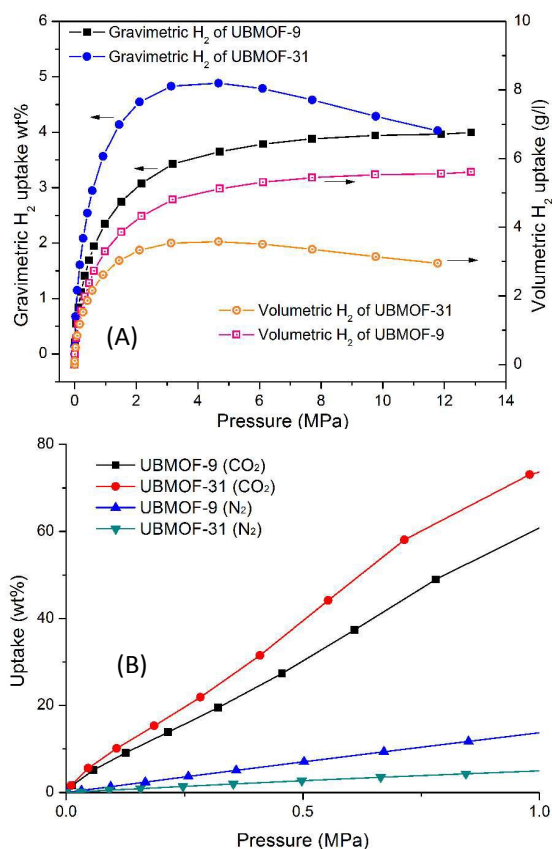


Figure 4. (A) High-pressure hydrogen adsorption studies (gravimetric and volumetric) for UBMOF-9 and UBMOF-31. (B) Study of CO₂ adsorption and N₂ adsorption showing greater affinity of UBMOF-31 for CO₂ over N₂, compared to UBMOF-9 at 1 MPa and 0 °C.

DASDCAH₂ linker to systematically investigate the effect of the amino group on hydrogen storage capacity for this family of Zr-based MOFs.

Acknowledgements

SN thanks Royal Society of Chemistry for financial support. VPT and UH thanks the University of Bath for funding through a Prize Research Fellowship and Whorrod Research Fellowship, respectively. MT thanks support from H2FC SUPERGEN Hub (EP/E040071/1). The Advanced Light Source is supported by the Director, Office of Science, Office of Basic Energy Sciences, of the U.S. Department of Energy under Contract No. DE-AC02-05CH11231

References

- 1 *Structure and Bonding (Fuel Cells and Hydrogen Storage)*, Springer, Heidelberg, Germany, 2011.
- 2 M. P. Suh, H. J. Park, T. K. Prasad and D. W. Lim, *Chem. Rev.*, 2012, **112**, 782-835.
- 3 M. Dincă and J. R. Long, *Angew. Chem. Int. Ed.*, 2008, **47**, 6766-6779.
- 4 C. Stockford, N. Brandon, J. Irvine, T. Mays, I. Metcalfe, D. Book, P. Ekins, A. Kucernak, V. Molkov, R. Steinberger-Wilckens, N. Shah, P. Dodds, C. Dueso, S. Samsatli and C. Thompson, *Int. J. Hydrogen Energ.*, 2015, **40**, 5534-5543.

- 5 J. L. C. Rowsell and O. M. Yaghi, *Angew. Chem. Int. Ed.*, 2005, **44**, 4670-4679.
- 6 H. W. Langmi, J. Ren, B. North, M. Mathe and D. Bessarabov, *Electrochim. Acta*, 2014, **128**, 368-392.
- 7 S. S. Han, J. L. Mendoza-Cortes and W. A. Goddard III, *Chem. Soc. Rev.*, 2009, **38**, 1460-1476.
- 8 L. J. Murray, M. Dinca and J. R. Long, *Chem. Soc. Rev.*, 2009, **38**, 1294-1314.
- 9 See the hydrogen storage target set by DOE in the United States <http://energy.gov/eere/fuelcells/downloads/fuel-cell-technologies-office-multi-year-research-development-and-22>
- 10 M. Dincă, A. Dailly, Y. Liu, C. M. Brown, D. A. Neumann and J. R. Long, *J. Am. Chem. Soc.*, 2006, **128**, 16876-16883.
- 11 Z. Wang, K. K. Tanabe and S. M. Cohen, *Chem. Eur. J.*, 2010, **16**, 212-217.
- 12 S. S. Kaye, A. Dailly, O. M. Yaghi and J. R. Long, *J. Am. Chem. Soc.*, 2007, **129**, 14176-14177.
- 13 J. H. Cavka, S. Jakobsen, U. Olsbye, N. Guillou, C. Lamberti, S. Bordiga and K. P. Lillerud, *J. Am. Chem. Soc.*, 2008, **130**, 13850-13851.
- 14 S. Chavan, J. G. Vitillo, D. Gianolio, O. Zavorotynska, B. Civalieri, S. Jakobsen, M. H. Nilsen, L. Valenzano, C. Lamberti, K. P. Lillerud and S. Bordiga, *Phys. Chem. Chem. Phys.*, 2012, **14**, 1614-1626.
- 15 L. Li, S. Tang, C. Wang, X. Lv, M. Jiang, H. Wu and X. Zhao, *Chem. Commun.*, 2014, **50**, 2304-2307.
- 16 Y. Han, H. Xu, Y. Liu, H. Li, H. Hou, Y. Fan and S. R. Batten, *Chem. Eur. J.*, 2012, **18**, 13954-13958.
- 17 J. Ren, N. M. Musyoka, H. W. Langmi, B. C. North, M. Mathe, X. Kang and S. Liao, *Int. J. Hydrogen Energ.*, 2015, **40**, 10542-10546.
- 18 J. Ren, H. W. Langmi, B. C. North, M. Mathe and D. Bessarabov, *Int. J. Hydrogen Energ.*, 2014, **39**, 890-895.
- 19 Isostructural compound to UBMOF-9 reported during reviewing process: R. J. Marshall, C. L. Hobday, C. F. Murphie, S. L. Griffin, C. A. Morrison, S. A. Moggach and R. S. Forgan, *J. Mater. Chem. A*, 2016, DOI: 10.1039/C5TA10401G; and in an MSc. thesis: <http://handle.ncl.edu.tw/11296/ndltd/48318579606892167335>.
- 20 O. V. Dolomanov, A. J. Blake, N. R. Champness and M. Schroder, *J. Appl. Crystallogr.*, 2003, **36**, 1283-1284.
- 21 S. B. Kalidindi, S. Nayak, M. E. Briggs, S. Jansat, A. P. Katsoulidis, G. J. Miller, J. E. Warren, D. Antypov, F. Corà, B. Slater, M. R. Prestly, C. Martí-Gastaldo and M. J. Rosseinsky, *Angew. Chem. Int. Ed.*, 2015, **54**, 221-226.
- 22 C. A. Trickett, K. J. Gagnon, S. Lee, F. Gándara, H.-B. Bürgi and O. M. Yaghi, *Angew. Chem. Int. Ed.*, 2015, **54**, 11162-11167.
- 23 R. C. Lochan and M. Head-Gordon, *Phys. Chem. Chem. Phys.*, 2006, **8**, 1357-1370.
- 24 L. Valenzano, B. Civalieri, S. Chavan, S. Bordiga, M. H. Nilsen, S. Jakobsen, K. P. Lillerud and C. Lamberti, *Chem. Mater.*, 2011, **23**, 1700-1718.
- 25 Determination of the specific surface area of powders – Part 1: BET method of gas adsorption for solids (including porous materials): BS 4359-1:1996, ISO 9277:1995 *Aerogels Handbook*, Springer-Verlag, New York, 2011.
- 26 U. Hintermair, C. Roosen, M. Kaefer, H. Kronenberg, R. Thelen, S. Aey, W. Leitner and L. Greiner, *Org. Process Res. Dev.*, 2011, **15**, 1275-1280.
- 28 N. Bimbo, J. E. Sharpe, V. P. Ting, A. Noguera-Díaz and T. J. Mays, *Adsorption*, 2013, **20**, 373-384.
- 29 T. M. McDonald, D. M. D'Alessandro, R. Krishna and J. R. Long, *Chem. Sci.*, 2011, **2**, 2022-2028.